

A Reconfigurable Frequency Selective Surface for Wi-Fi Application

Thamyris da Silva Evangelista¹ , Deisy Formiga Mamedes² , Jefferson Costa e Silva³ ,

Alexandre Jean René Serres¹ , Alfredo Gomes Neto³ 

¹Federal University of Campina Grande, UFCG, Paraíba, Brazil

thmyris.evangelista@ee.ufcg.edu.br, alexandreserres@dee.ufcg.edu.br

²Department of Electrical and Computer Engineering, University of Victoria, UVic, British Columbia, Canada
mamedes@uvic.ca

³Group of Telecommunications and Applied Electromagnetism, GTEMA

Federal Institute of Paraíba, IFPB, Paraíba, Brazil

jefferson@ifpb.edu.br, alfredogomes@ifpb.edu.br

Abstract— This work presents the development of a reconfigurable frequency selective surface (RFSS) for application in the 2400-2483.5 MHz band, standard IEEE 802.11b/g/n (Wi-Fi). The proposed RFSS is based on the four-arms star geometry and PIN diodes were used as switching elements. In the initial design, numerical and measured results, especially for *y* polarization, PIN diode on-state, shown a difference of 15% for the resonant frequency. To overcome this drawback, a scaling factor was adopted and RFSS was redesigned and characterized, achieving the desired frequency response. The RFSS reconfigurability is confirmed, with a variation of at least 15 dB, when switching the states of the PIN diode. Moreover, the signal strength was measured directly on a notebook, confirming the reconfiguration of the RFSS. Finally, for the *y* polarization, it was found that for this polarization the frequency response remains virtually unchanged, even for angles of incidence up to 45°. In addition to the Wi-Fi signal control, the observed features make the developed RFSS especially attractive for reconfigurable antennas applications.

Index Terms— Reconfigurable frequency selective surface, RFFS, four-arms star, PIN diode, IEEE 802.11b/g/n, Wi-Fi.

I. INTRODUCTION

With the proliferation of wireless communications devices, the demand for signal coverage, network capacity, privacy of communications, and user quality of service, particularly in densely populated areas, poses a challenge for RF/Microwave engineers. On the other hand, there are applications where it may be appropriate to block or shield communications such as in prisons, military buildings, embassies, and hospitals [1]-[4]. It is still necessary to consider that wireless communication environment in indoor locations is adversely affected by multipath reflection interferences [5]-[8]. Therefore, each wireless communication environment, with its specific characteristics, requires different propagation solutions. Frequency selective surfaces (FSSs) have been widely used to reach specific requirements in different wireless communication environment [1],

[2].

FSSs are generally periodic structures formed by patch or aperture elements etched on a dielectric substrate, designed to reflect, transmit or absorb electromagnetic (EM) waves. FSSs can pass or block the waves of certain frequencies in free space, providing filtering properties, hence, they are also known as spatial filters. The FSS frequency response may present band-reject or band-pass characteristics, according to its type of element being patch or aperture, respectively. Parameters such as substrate thickness (h) and relative dielectric permittivity (ϵ_r), basic cell dimensions, element geometry and its periodicity, Fig. 1, determine the FSS frequency response, [9], [10]. In recent years, considering characteristics such as diversity of applications, low cost of fabrication, reduced weight and volume, ease of integration with other parts of telecommunication systems, FSSs have attracted the attention of many research groups.

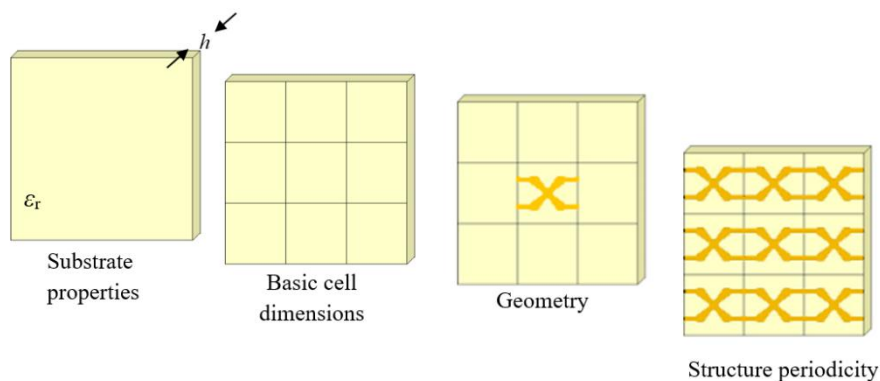


Fig. 1. Parameters that affect the FSS frequency response.

In several wireless applications, in accordance with the field strength, or the communication quality, it is desired to modify the propagation characteristics. In this case, the use of a reconfigurable FSS (RFSS) has demonstrated a good approach. An RFSS is an FSS for which the frequency response can be modified by electronic [1], [11], [12] or mechanical [5], [13], [14] means.

The aim of this paper is to present the development of an RFSS, operating in the 2400-2483.5 MHz frequency band, which includes the IEEE 802.11b/g/n (Wi-Fi) standards. The RFSS proposed in this paper is based on four-arms star geometry, having its reconfigurability by using PIN diodes, [15], [16].

This paper is organized as follow. After this Introduction, the design of the proposed RFSS is described in Section II. Numerical and measured results are presented in Section III. Conclusions are drawn in Section IV.

II. RFSS DESIGN

The four-arms star geometry, Fig. 2, was firstly presented in [15] for switchable applications and modifications were performed for other applications throughout the years [16]-[19]. The design procedure to obtain this geometry is detailed in [18], [19]. Without the gap, the four-arms star geometry can be symmetric and its frequency response is polarization independent. When the gap is introduced, the frequency response becomes polarization dependent, with a great variation for the

polarization perpendicular to the gap, y polarization (Fig. 2(b)). For the polarization parallel to the gap, x polarization in Fig. 2(b), the frequency response remains practically unchanged. However, with the insertion of bias lines the x polarization is affected, [16].

Without the gap, the FSS resonant frequency can be approximately determined by (1), with good results, principally for $h \ll \lambda_0$, [18], [19].

$$f_{res}(GHz) = \frac{0.3}{2L_{eff}}, \quad (1)$$

in which $L_{eff} = Lx + Ly$.

Considering the y polarization, with the gap and the bias lines, the resonant frequency, f_{res-gb} , can be estimated by (2), [16].

$$1.5f_{res} \leq f_{res-gb}(GHz) \leq 2.0f_{res}, \quad (2)$$

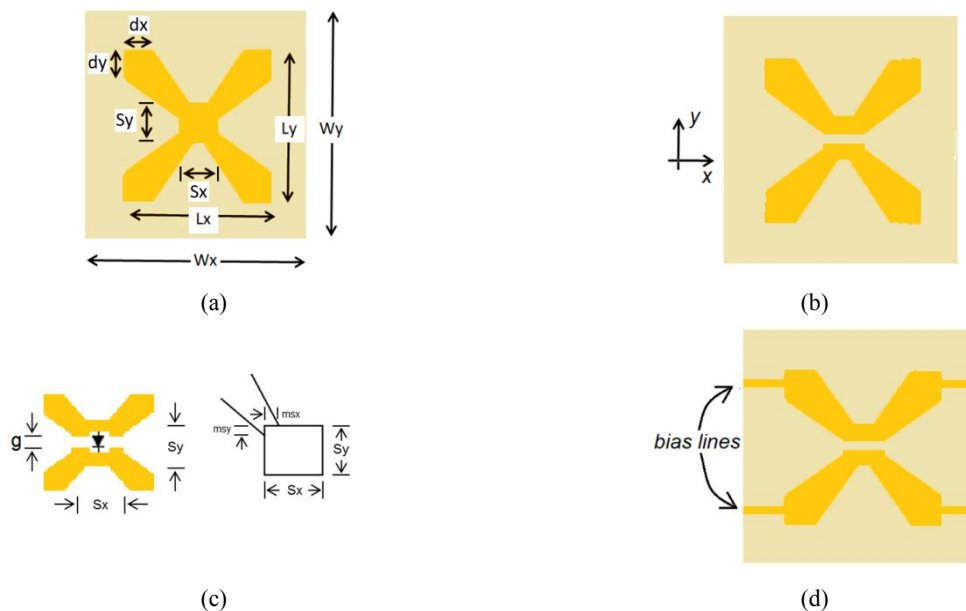


Fig. 2. Four-arms star geometry. (a) Geometry dimensions, without gap, (b) Geometry with gap, (c) Gap details, (d) Geometry with gap and bias lines.

After the basic cell design, an RFSS with a total number of 36 basic cells, with 6×6 elements was fabricated, Fig. 3. Note that each cell line can be controlled individually, which is very interesting, both in the manufacturing process and in the RFSS test process.

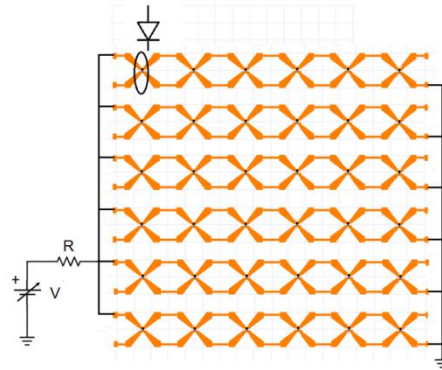


Fig. 3. RFSS, with 6 lines, each one with 6 basic cells.

III. NUMERICAL AND MEASURED RESULTS

Simulations were performed using ANSYS Electronics Desktop [20]. The RFSS was designed on a low-cost fiberglass dielectric substrate (FR-4) with relative dielectric permittivity $\epsilon_r = 4.4$, substrate thickness $h = 1.6 \text{ mm}$ and loss tangent $\tan(\delta) = 0.02$. The RFSS was built on a board measuring $240 \text{ mm} \times 230 \text{ mm}$, as shown in Fig. 4. The SMP1340-0769LF PIN diode was used [21] as active element device.

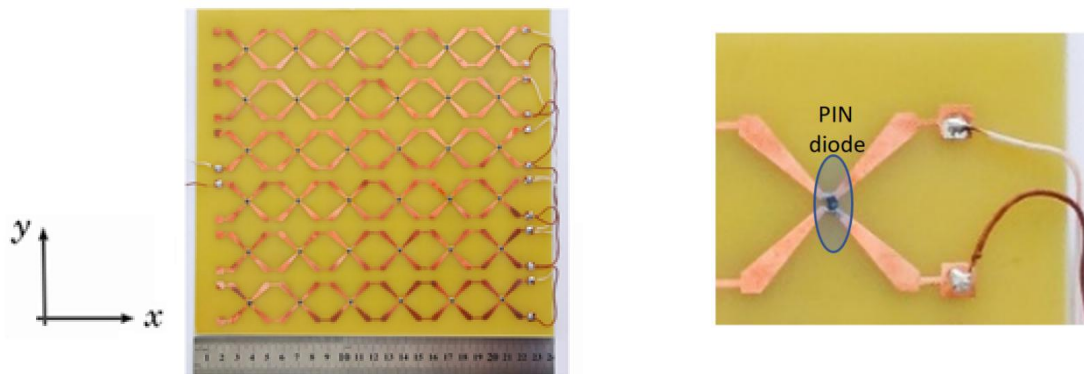


Fig. 4. Manufactured RFSS with inserted PIN diode and bias lines connection points.

The measurements were carried out using a VNA Agilent E5071C [22], two double ridge guide A. H. Systems antennas, model SAS-571[23], and a measurement window. The measurement setup is shown in Fig. 5 for RFSS with PIN diode. In this case, a 150Ω resistor was used to limit the current in the diodes. In the numerical simulation and in the experimental results, the x and y polarizations were considered, with incident electromagnetic wave normal to the RFSS. Numerical and experimental results are presented considering the frequency range from 2.0 GHz to 10.0 GHz.

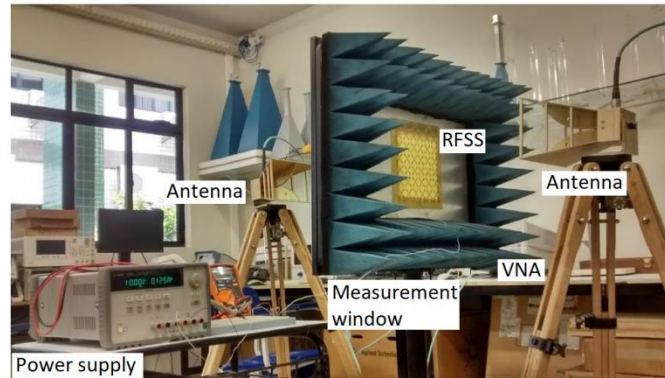


Fig. 5. Measurement setup.

The FSS fabrication is determined by two main points: desired frequency response and fabrication process constraints. As a first approach, the frequency response can be estimate by equations (1) and (2). It is a first step to be followed by a numerical optimization. However, this can be easily accomplished.

The FSS prototype presented in this paper was fabricated using a PCB “homemade” process, in which geometry is printed on an adhesive and it is attached to the substrate surface. Then, the metallic surface that is not part of the FSS is removed by corrosion in iron perchloride. In our case, this process limits the dimensions to a minimum value of 1 mm.

Considering the previous statements, as an initial design, the dimensions of the designed basic cell geometry are depicted in Fig. 6. Note that for numerical simulations, ideal PIN diodes are assumed, and the on-state is represented by a metallic strip connecting the gap sides. The gap itself represents the ideal PIN diode off-state.

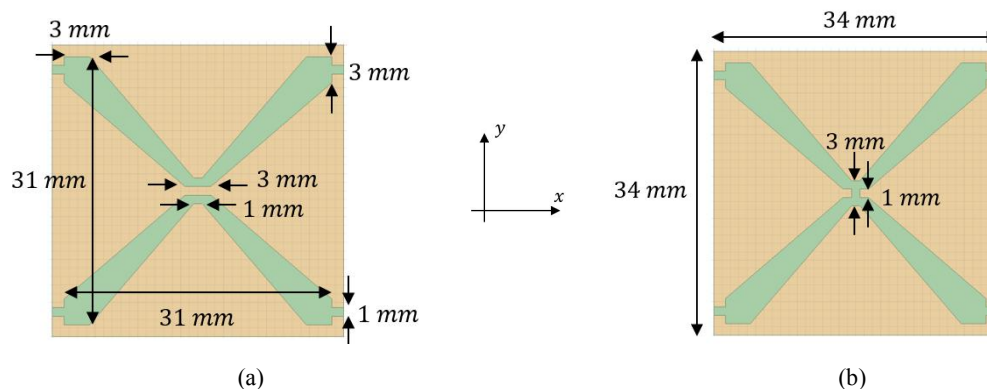


Fig. 6. Dimensions of the FSS basic element cell, initial design. (a) Four-arms star, ideal off-state, first try, (b) Four-arms star, ideal on-state

Fig. 7 shows the simulated results for each step described in Fig. 2, considering the dimensions depicted in Fig. 6. As for the numerical results the desired RFSS frequency response was achieved, a prototype was fabricated and experimentally characterized. The obtained results are presented in Fig. 8, with at least 20 dB of difference between on-state ($V = 2.0V$) and off-state ($V = 0.0V$), at the resonant frequency, 2.2 GHz.

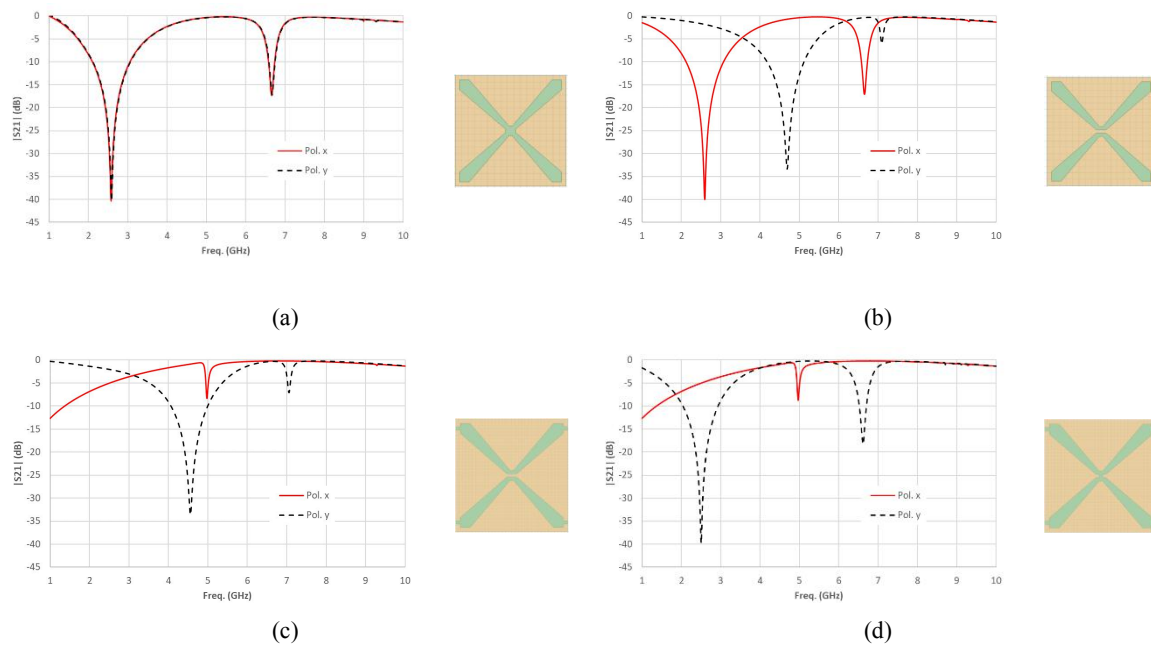


Fig. 7. Dimensions of the FSS basic element cell, initial design. (a) Four-arms star, in accordance with (1), $L_x = L_y = 31 \text{ mm}$, $f_{res} = 2.58 \text{ GHz}$, (a) Four-arms star, in accordance with (1), $L_x = L_y = 31 \text{ mm}$, $f_{res} = 2.58 \text{ GHz}$, (b) Four-arms star with gap, $L_x = L_y = 31 \text{ mm}$, $f_{res-pol. x} = 2.58 \text{ GHz}$, $f_{res-pol. y} = 4.69 \text{ GHz}$, (c) Four-arms star with gap and bias lines, $L_x = L_y = 31 \text{ mm}$, $f_{res-pol. y} = 4.56 \text{ GHz}$ (c) Four-arms star with gap and bias lines, $L_x = L_y = 31 \text{ mm}$, $f_{res-pol. y} = 4.56 \text{ GHz}$, (d) Four-arms star with metallic strip and bias lines, $L_x = L_y = 31 \text{ mm}$, $f_{res-pol. y} = 2.51 \text{ GHz}$

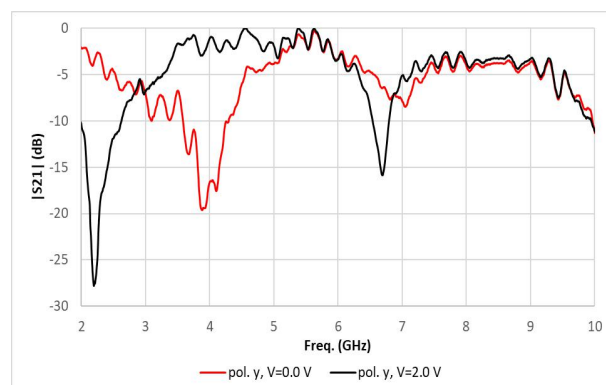


Fig. 8. Frequency response, y polarization, measured results for the RFSS initial design.

Despite the achieved reconfigurability, 20 dB, the resonant frequency, 2.2 GHz, was out of the range of interest, 2.4 GHz. It must be highlighted that after the measured results, new simulations were performed, modifying the PIN diode model, considering equivalent lumped elements to describe on-state and off-state, but the numerical results remained unsatisfactory when compared to measured ones. One possible reason for this discrepancy is that the RFSS simulation is performed using Floquet ports, which impose an infinite periodicity and only one basic cell is simulated. Furthermore, the insertion of an RF choke after the DC power supply did not affect measured results significantly.

After exhausting the available numerical procedures, the option was to redesign the RFSS project, scaling the dimensions according to the difference between the measured resonant frequencies, 2.2 GHz, and the simulated ones, 2.5 GHz. In this way, a new value of $L_x = L_y = 27 \text{ mm}$ was determined and the results obtained will be detailed below. Dimensions of the after scaling FSS are depicted in Fig. 9.

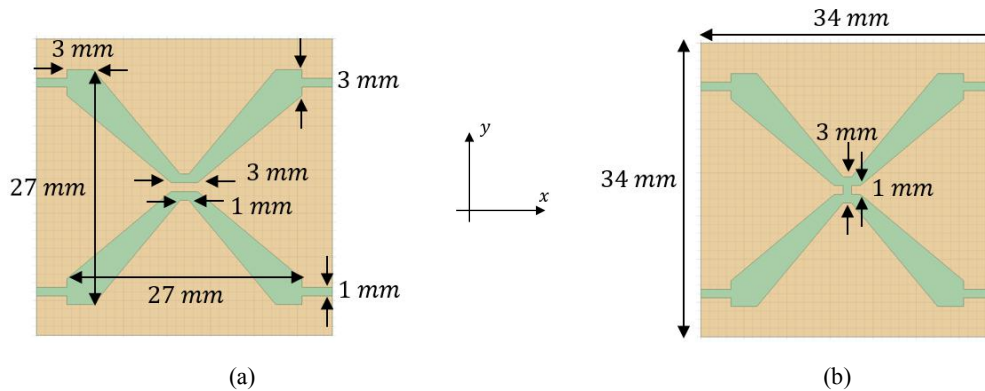


Fig. 9. Dimensions of the FSS basic element cell, after scaling. (a) Four-arms star, ideal off-state, (b) Four-arms star, ideal on-state

A. X polarization

In Fig. 10 it can be observed the frequency responses for RFSS considering the ideal off-state, before inserting the PIN diode. A good agreement is observed between numerical and measured results. The difference observed at the beginning of the frequency range are due to the limitations of the measurement process, when the wavelength is relatively large compared to the dimensions of the measurement window and the gain of the antennas is low.

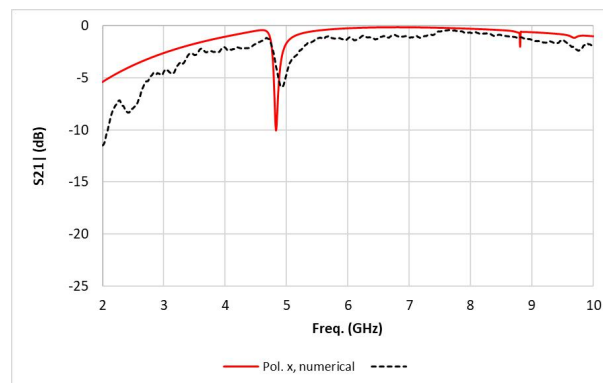


Fig. 10. Frequency response, x polarization, ideal off-state.

After analyzing the behavior of the FSS for the ideal off-state, PIN diodes were inserted and the obtained result is presented in Fig. 11, verifying a good agreement between numerical and measured results. In Fig. 12, measured results for different PIN diodes polarization states: 0.0 V (off-state), 0.8 V (transition region) and 1.8 V (on-state) are presented. As expected, the frequency responses remain practically the same. The Table I summarizes the obtained results.

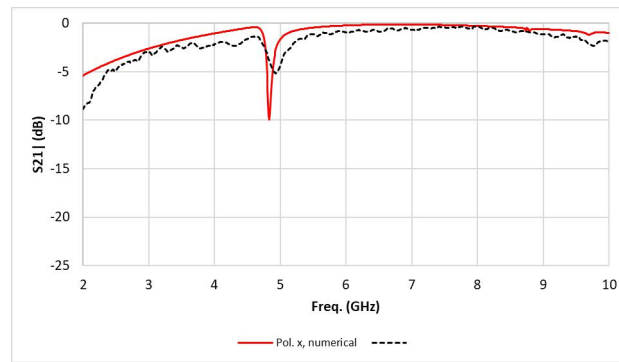


Fig. 11. Frequency response, x polarization, PIN diode off-state.

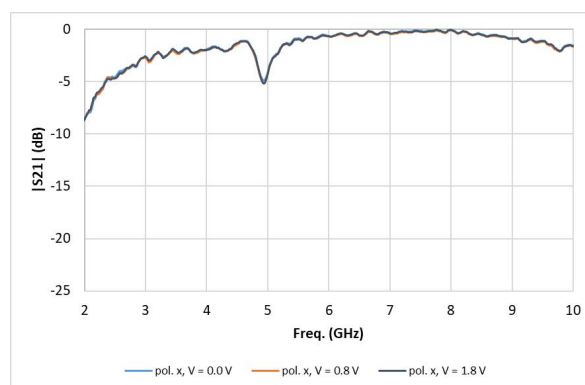


Fig. 12. Frequency response, x polarization, for different PIN diode polarization states.

TABLE I – RESULTS FOR X POLARIZATION

Types of RFSS		Frequency (GHz)		Difference (%)
		Numerical	Measured	
FSS without Diodes	Off - Ideal	4.83	4.96	2.69
	On - Ideal	4.83	—	—
FSS with Diodes	Off	—	4.94	—
	Transition	—	4.94	—
	On	—	4.94	—

B. Y polarization

Analogously to the x polarization, for the y polarization the FSS was characterized considering the ideal off-state, and the obtained results are presented in Fig. 13. Once again, a good agreement is verified between numerical and measured results. The Table II summarizes the obtained results.

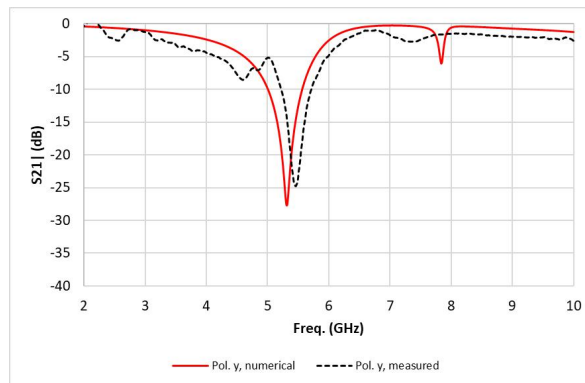


Fig. 13. Frequency response, y polarization, ideal off-state.

In Fig. 14 the frequency responses for the RFSS considering the PIN diode in the on-state are presented. The simulated resonant frequency was 2.78 GHz and the measured one 2.42 GHz, presenting a difference of 14.87%, corresponding to the adopted scaling factor. It is also noteworthy that the resonant frequency calculated using (1) is 2.78 GHz, practically the same value considering the ideal model in the simulation.

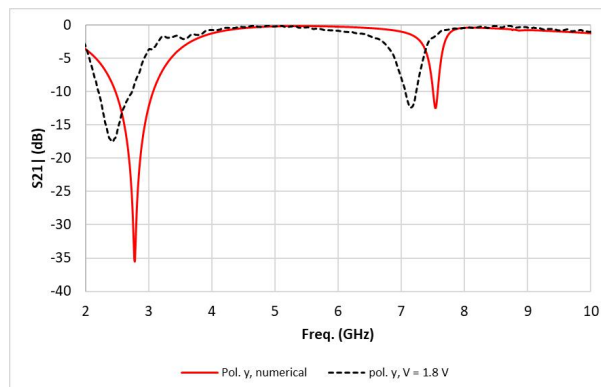


Fig. 14. Frequency response, y polarization, PIN diode in on-state.

TABLE II – RESULTS FOR Y POLARIZATION.

Types of RFSS		Frequency (GHz)		Difference (%)
		Numerical	Measured	
FSS without Diodes	Off - Ideal	5.31	5.46	2.82
	On - Ideal	2.78	—	—
FSS with Diodes	Off	—	4.39	—
	Transition	—	—	—
	On	—	2.42	—

The characterization of the FSS, in the y polarization, was also done with different voltage levels being applied to the PIN diodes. In Fig. 15 the results for 0.0 V, 0.8 V and 1.8 V are presented. From the achieved results, it can be highlighted that at the frequency of interest, 2.42 GHz, it was possible to obtain a variation greater than 15 dB, for a switching from the off-state to the on-state. Furthermore, in the transition region, in the considered frequency range, practically the RFSS does not present any resonant frequency, a result in accordance to [18], which is a very attractive feature for some applications.

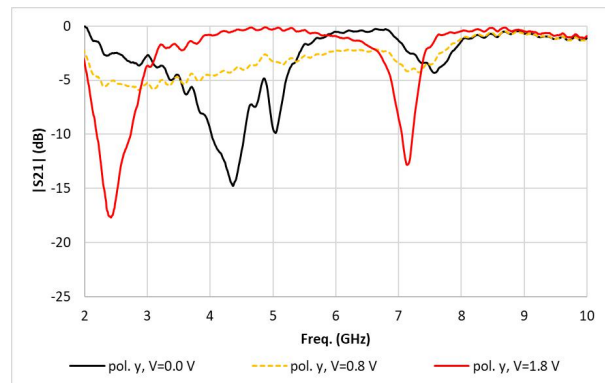


Fig. 15. Frequency response, polarization y , for different PIN diode polarization states.

C. Wi-Fi Signal Strength Measurements

In order to measure the Wi-Fi signal strength, in the range of 2400-2483.5 MHz, the measurement setup depicted in Fig. 16 was employed. Basically, it is composed of the developed RFSS, a power supply, the measurement window, a notebook and a Yagi-Uda AMXY-2400-16 antenna [23], with 16 elements, (2400 - 2483 MHz) and 16 dBi gain. The antenna is directly connected to an Internet access point, replacing its original antenna. The Wi-Fi signal strength is monitored with Homedale software [24], installed in the notebook. For these measurements, only the y polarization was considered.

In Fig. 17 and 18 is illustrated the signal strength obtained using the monitoring software. Initially the PIN diodes are in the off-state, so the RFSS does not attenuate the Wi-Fi signal. Upon switching to the on-state, the Wi-Fi signal has an attenuation of at least 20 dB, which is a result quite interesting, thus confirming the reconfiguration of the FSS.

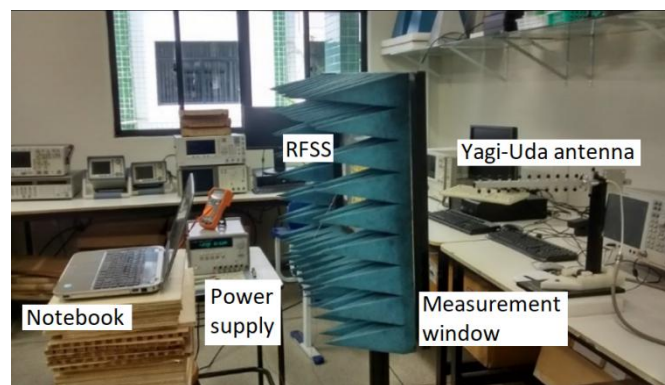


Fig. 16. Wi-Fi field strength measurement setup.



Fig. 17. Wi-Fi signal strength response displayed on notebook, y polarization..

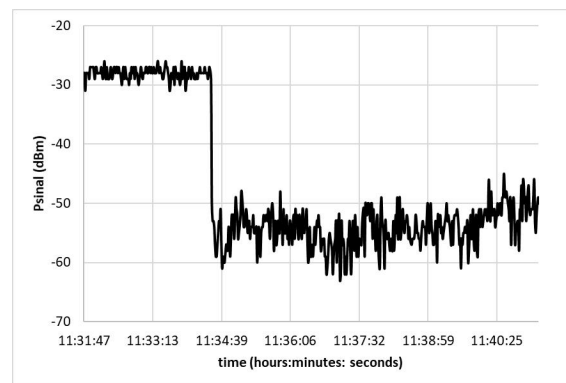


Fig. 18. Wi-Fi signal strength response, y polarization..

D. Angular Dependency

Measurements were also performed taking into account the angular dependency for oblique incidence of plane waves. In this case, only the y polarization was considered, since in the x polarization the frequency response is not affected by the change of on- and off-states.

Frequency responses for an incidence angle of 0° , 15° , 30° and 45° are presented in Fig. 19 for the RFSS in off-state, with an applied voltage 0.0 V. Considering the normal incidence ($\theta = 0^\circ$) as the reference, the resonant frequencies present differences of 0.91% , 8.25% , 17.43%, for $\theta = 15^\circ$, 30° and 45° , respectively. However, no resonance appears in the frequency range of interest (2.4 GHz). In a similar way, results are presented for on-state, with an applied voltage of 1.8 V, in Fig. 20. The resonant frequencies present differences of 2.41% , 2.01% , 1.61%, for $\theta = 15^\circ$, 30° and 45° , respectively. In this case, even for an incidence angle of 45° , there is practically no variation in the resonant frequency, indicating good angular stability. Table III summarizes the obtained results.

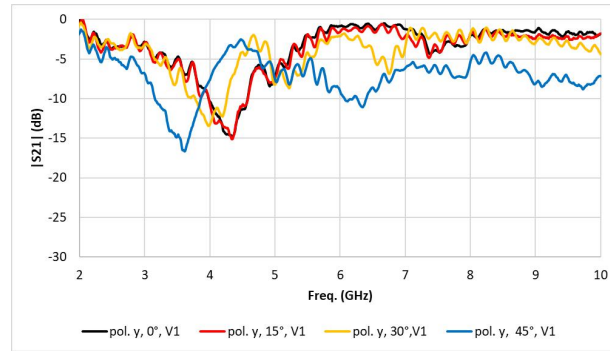


Fig. 19. Frequency response for angular variation, y polarization, PIN diode off-state, $V_1 = 0.0$ V.

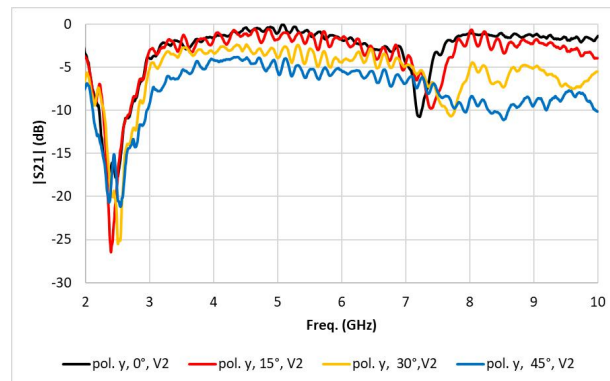


Fig. 20. Frequency response for angular variation, y polarization, PIN diode on-state, $V_2 = 1.8$ V.

TABLE III – MEASURED RESONANT FREQUENCY

Incidence angle	Off-state (GHz)	On-state (GHz)
0°	4.36	2.48
15°	4.32	2.42
30°	4.00	2.53
45°	3.60	2.52

IV. CONCLUSIONS

This work presented the development and characterization of a reconfigurable frequency selective surface, RFSS, based on the four-arms star geometry, using the PIN diode as a switching element for application in the 2400-2483.5 MHz band of the IEEE 802.11 b/g/n (Wi-Fi).

After a brief description of the four-arms star geometry, the FSS design procedure, including initial equations, was described. Inserting the PIN diode ideal model, the RFSS was obtained and numerically and experimentally characterized. However, for the measured results, despite the good reconfigurability, 20 dB, the resonance frequency, 2.2 GHz, was out of desired frequency range, 2.4 GHz. Even improving the PIN diode model or adding an RF choke between the power supply and the RFSS, numerical results were not satisfactory when compared to measured ones, with a difference of 15%. Then, a scaling factor was adopted and a new RFSS was designed and characterized.

Considering the new RFSS, with $L_x = L_y = 27$ mm, for x polarization, it was verified that switching the PIN diode, from off-state to on-state, does not change the frequency response of the

RFSS, which is expected, considering that the electric field is practically null in the switching region for this polarization. The RFSS characterization was done for different voltage levels being applied to the PIN diode (0.0 V, off-state, 0.8 V, transition region, and 1.8 V, on-state), observing a good agreement between numerical and measured results.

Analogously, for the y polarization, the RFSS characterization was done for the same voltage levels. Once again, the numerical result for the resonant frequency, 2.78 GHz, was 15% greater than the measured one, 2.42 GHz, proving the effectiveness of the adopted scale factor. For the desired frequency band, 2.4 GHz, it has been achieved an attenuation of at least 15 dB, for the PIN diodes switching states. Furthermore, the effect of the PIN diode transition region, when the RFSS gets almost transparent was observed.

The Wi-Fi signal strength was measured directly on a notebook using Homedale software and the results were quite satisfactory, confirming the reconfigurability of the developed RFSS, with an attenuation of at least 20 dB.

Finally, the developed RFSS was characterized for different incidence angles ($\theta = 0^\circ, 15^\circ, 30^\circ$ and 45°) and it was observed that for the y polarization the frequency response remains virtually unchanged, even for angles of incidence up to 45° .

Concluding, it must be also highlight that, in addition to signal strength control, the developed RFSS is a promising structure for other applications, especially reconfigurable antennas.

ACKNOWLEDGMENT

This work was partially supported by the Federal Institute of Paraíba Graduate Program in Electrical Engineering (PPGEE-IFPB) and the Federal University of Campina Grande Graduate Coordinator in Electrical Engineering (COPELE/UFCG).

REFERENCES

- [1] R. Panwara, J. R. Lee, "Progress in frequency selective surface-based smart electromagnetic structures: A critical review," *Aerospace Science and Technology*, vol. 66, pp. 216–234, 2017.
- [2] A. Kapoor, R. Mishra, P. Kumar, "Frequency selective surfaces as spatial filters: Fundamentals, analysis and applications," *Alexandria Engineering Journal*, vol. 61, pp. 4263–4293, 2022.
- [3] J. Roberts, K. L. Ford, and J. M. Rigelsford, "Secure electromagnetic buildings using slow phase-switching frequency-selective surfaces," *IEEE Trans. Antennas Propagation*, vol. 64, no. 1, pp. 251–260, Jan. 2016.
- [4] X. Xiong, and W. Hong, "WiFi band-stop FSS for increased privacy protection in smart building," in *Proc. 2015 IEEE 6th International Symposium on Microwave, Antenna, Propagation, and EMC Technologies (MAPE)*, Shanghai, China, Oct. 2015, pp. 826–828.
- [5] D. Ferreira, I. Cuiñas, R. F. S. Caldeirinha, and T. R. Fernandes, "3-D Mechanically tunable square slot FSS," *IEEE Trans. Antennas Propagation*, vol. 65, no. 1, pp. 242–250, Jan. 2017.
- [6] S. Cho, I. Lee and I. Hong, "Frequency selective film design for building walls for blocking wireless LAN signal," *2018 International Symposium on Antennas and Propagation (ISAP)*, Busan, Korea (South), 2018, 23–26 Oct. 2018, pp. 1–2.
- [7] K. Nakamura, and Y. Okano, "Design of functional wall considering oblique incidence," in *Proc. 2017 IEEE International Symposium on Radio-Frequency Integration Technology (RFIT)*, Seoul, Korea, Aug. 30–Spt. 01, 2017, pp. 104–106.

- [8] S. Habib, G. I. Kiani, and M. F. U. Butt, "Interference mitigation and WLAN efficiency in modern buildings using energy saving techniques and FSS," in *Proc. 2016 IEEE International Symposium on Antennas and Propagation (APSURSI)*, Fajardo, Puerto Rico, Jun. 26-Jul 01, 2016, pp. 965-966.
- [9] B. A. Munk, *Frequency Selective Surfaces - Theory and Design*, New York: Wiley, 2000.
- [10] T. K. Wu, *Frequency Selective Surface and Grid Array*, John Wiley & Sons, INC., New York, 1995.
- [11] F. Samadi and A. Sebak, "Reconfigurable surface design for electromagnetic wave control," *2019 IEEE International Electromagnetics and Antenna Conference (IEMANTENNA)*, Vancouver, BC, Canada, 09 December 2019, pp. 025-028,
- [12] Q. Guo, Z. Li, J. Su, J. Song and L. Y. Yang, "Active frequency selective surface with wide reconfigurable passband," in *IEEE Access*, vol. 7, pp. 38348-38355, 2019.
- [13] R. Sivasamy, B. Moorthy, M. Kanagasabai, V. R. Samsingh, and M. G. N. Alsath, "A wideband frequency tunable FSS for electromagnetic shielding applications," *IEEE Transactions on Electromagnetic Compatibility*, vol. 60, no. 1, pp. 280-283, February 2018.
- [14] S. Abirami, E. F. Sundarsingh and V. S. Ramalingam, "Mechanically reconfigurable frequency selective surface for RF shielding in indoor wireless environment," in *IEEE Transactions on Electromagnetic Compatibility*, vol. 62, no. 6, pp. 2643-2646, Dec. 2020.
- [15] A. Gomes Neto, J. N. de Carvalho, A. N. da Silva, H. de P. A. Ferreira, I. S. S. Lima, J. I. Fernandes, "Four arms star: an useful geometry for switchable FSS," in *2013 SBMO/IEEE MTT-S International Microwave and Optoelectronics Conference (IMOC)*, Rio de Janeiro, Brazil, Aug. 2013, pp. 1-5.
- [16] A. Gomes Neto, J. C. e Silva, A. G. Barboza, I. B. G. Coutinho, M. de O. Alencar, M. C. de Andrade, "Modeling the resonant behavior of continuously reconfigurable FSS based on four arms star geometry," *Journal of Microwaves and Optoelectronics*, v. 19, p. 415-427, 2020.
- [17] A. Gomes Neto, J. C. e Silva, J. N. de Carvalho, A. P. da Costa, L. C. M. de Moura, "Bandpass frequency selective surface using asymmetrical slot four arms star geometry," *Microwave and Optical Technology Letters*, v. 58, p. 1105-1109, 2016.
- [18] D. F. Mamedes, A. G. Neto, J. C. e Silva, and J. Bornemann, "Design of reconfigurable frequency-selective surfaces including the PIN diode threshold region," *IET Microw., Antennas Propag.*, vol. 12, no. 9, pp. 1483-1486, 2018.
- [19] A. G. Neto, J. C. e Silva, A. G. Barboza, D. F. Mamedes, I. B. G. Coutinho and M. de Oliveira Alencar, "Varactor-tunable four arms star bandstop FSS with a very simple bias circuit," *2019 13th European Conference on Antennas and Propagation (EuCAP)*, Krakow, Poland, 2019, pp. 1-5.
- [20] <https://www.ansys.com/products/electronics>
- [21] https://www.skyworksinc.com/-/media/SkyWorks/Documents/Products/101-200/SMP1340_Series_200051U.pdf
<https://www.keysight.com/br/pt/product/E5071C/e5071c-ena-vector-network-analyzer.html>
- [22] <https://www.ahsystems.com/catalog/SAS-571.php>
- [23] <http://www.ameison-antenna.com/sale-8844685-2-4ghz-16bi-aluminium-high-performance-wifi-yagi-antenna-wireless-wlan-antenna.html>.
- [24] <https://homedale.br.uptodown.com/windows>.
- [25] Yagi antenna [Online]. Available: <http://www.ameison-antenna.com/sale-8844685-2-4ghz-16bi-aluminium-high-performance-wifi-yagi-antenna-wireless-wlan-antenna.html>. [Access in 30 june 2021].